IEEE Access
Multidisciplinary ⋮ Rapid Review ⋮ Open Access Journal

Received 27 July 2024, accepted 10 August 2024, date of publication 13 August 2024, date of current version 23 August 2024.

Digital Object Identifier 10.1109/ACCESS.2024.3443025

RESEARCH ARTICLE

AAN Controller With Adaptive Gain for Upper Limb Exoskeleton

JIXIN DONG[1,2], ZHIWEI JIA[1,2], ERWEI LI[1,2], AND QIPENG LV[3]

[1]Hebei Provincial Key Laboratory of Parallel Robot and Mechatronic System, Yanshan University, Qinhuangdao 066004, China
[2]Key Laboratory of Advanced Forging & Stamping Technology and Science, Ministry of Education of China, Yanshan University, Qinhuangdao 066004, China
[3]Second Research Institute of China Electronics Technology Group Corporation, Taiyuan 030024, China

Corresponding author: Erwei Li (lierwei@ysu.edu.cn)

This work was supported by the National Key Research and Development Program Projects of China under Grant 2019YFB1312502.

ABSTRACT In this paper, the problem of the assist-as-needed (AAN) control of the upper limb exoskeleton is studied. Due to the complexity of the upper limb exoskeleton structure and driving mode, the control parameters of the equipment need to be adjusted to obtain satisfactory control performance. This paper presents an adaptive gain control method based on AAN. Through the dynamic gain adjustment mechanism, the system can adjust the control force in real-time to avoid excessive or insufficient auxiliary force. It can overcome the problem that traditional adaptive cannot identify dynamically changing parameters efficiently, and effectively avoid the overshoot and oscillation problems of high-gain adaptive, and do not need to obtain unknown disturbance information in complex models. The method adopts the on-demand auxiliary strategy to realize the self-adaptation of the auxiliary force and mode adjustment, which ensures the comfort, safety and effectiveness in the rehabilitation process. Through simulation experiment and comparison with the latest AAN controller, it can be seen that the controller has good anti-jamming effect and adaptive adjustment ability to auxiliary force under unknown interference.

INDEX TERMS Adaptive control, AAN control, cable-driven upper limb exoskeleton.

I. INTRODUCTION

The recovery of the affected upper limb function has always been one of the difficulties in stroke rehabilitation [1]. Enhancing motor function in stroke patients has become an important goal of therapists' work [2]. In recent years, robot-assisted rehabilitation of upper limb rehabilitation, as a new form of rehabilitation, has gradually replaced manual-assisted training, saved a lot of clinical medical resources, and made rehabilitation training develop intelligently, which has achieved the rehabilitation of some stroke patients [3], [4].

Common upper limb rehabilitation robots are mainly divided into two categories: exoskeleton robots and end traction robots. The terminal traction robot has a relatively simple structure through single-point contact and interaction with the patient's hand or forearm. Exoskeleton robots can achieve individual joint control while avoiding singularities [5]. For example, MGA [6], ANYexo [7], etc., when the drivers are placed at the joint, the volume and mass of the worn part increase compared with the movement inertia of the patient, and the comfort is reduced. Rod-driven exoskeleton has the advantage of being lightweight. In recent years, the emergence of rod-driven exoskeletons such as ARMin [8], CADEN [9] and ShoulderRO [10] has made its application in the field of rehabilitation more extensive.

The controller of the rehabilitation robot is one of the key factors to ensure its rehabilitation treatment effect and safety. Most controllers are designed to strictly track the desired motion pattern. This controller is suitable for individuals with severe impairment of function; however, this excessive intervention is not as effective in the rehabilitation of patients with partial motion [11]. In recent years, a controller that provides minimal auxiliary force to the patient has been proposed called the assist-as-needed (AAN) controller. Some controllers adjust the impedance parameters by the error of the observed quantity to reflect the AAN [12]. Others adjust the output of the controller directly by the error of the observed quantity to achieve the AAN objective [13]. For

The associate editor coordinating the review of this manuscript and approving it for publication was Diego Oliva.

example, this paper designs a new adaptive hybrid mode on Demand (AHMAAN) control algorithm, in which the hybrid mode consists of resistance mode and auxiliary mode and embodies AAN characteristics through the designed adaptive gain factor [14]. An on-demand assist (ATAAN) impedance control based on active torque is proposed, and modulated according to the approximate value of the active torque and the position error of the patient to achieve the on-demand assist characteristics [15]. An upper limb exoskeleton Adaptive Assistance on Demand (TTP-AAAN) control algorithm based on training task planning reflects AAN characteristics by adjusting the training difficulty according to the patient's intention and performance [16].

In addition, to the complexity of the exoskeleton nonlinear dynamics model, it is more difficult to achieve accurate control of the exoskeleton [17]. Scholars have proposed various methods to guarantee the robustness and stability of complex systems [18], [19]. The back-stepping method is often used in controllers to compensate for uncertain disturbances. The performance of controllers is affected by the upper limit of time-varying disturbance, which makes the tracking error difficult to converge. Before the experiment, the selection of the parameters of the equipment is accidental, so the selection and adjustment of the parameters need a long process, and only the correct parameters can get satisfactory control performance. The constant value of a stable gain at one time cannot guarantee the ideal control performance of the system under the influence of time-varying perturbations. Therefore,the self-tuning control algorithm is designed to solve the control parameter tuning problem, but this kind of control algorithm does not consider the time-varying interference, and it is difficult to achieve the expected control performance.

High-gain techniques are often used to achieve accurate and robust control performance. BLF-based Barrier Lyapunov function (Barrier Lyapunov function, BLF) controller has been designed to ensure that the tracking error reaches the desired control performance. When the tracking error reaches a certain range boundary, the controller gain is adjusted to infinity to prevent it from going beyond the boundary [20]. A controller based on a specified performance function (PPF) uses a reversible performance function for error transformation to obtain a specified transient and steady-state performance [21]. Although the above controller can meet the expected control requirements, it needs to ensure that the error is within a certain range. When the disturbance is too large or when the tracking error exceeds the limit, the system may become unstable. Selecting the gain of the interference observer (DO) by obtaining information on the maximum frequency of interference, and thus accurately estimating performance for use with BLF or PPF control methods have been developed for industrial use [22], [23]. However, the uncertainty of the maximum frequency results in observer gains usually obtained by trial and error.

The common feature of tracking problems of complex nonlinear systems solved by the above methods is that the boundedness of tracking errors depends on the upper bounds of unknown interference and control/observer gain, so the external tracking error disturbance can be reduced by high gain. However, unnecessary high gain may cause amplification of high-frequency measurement noise, so peak phenomena due to the multiplication of high gain and initial error should be avoided [24]. It is difficult for the above method to select the appropriate control gain to obtain satisfactory control performance without interference information. Therefore, it is necessary to study a gain adaptive control method without interfering with information on the premise of avoiding high gain.

At present, there are few researchers related to the above problems. A scale-integral-derivative (PID) gain self-tuning method based on sliding mode dynamic gradient descent is developed [25]. In addition, according to the relationship between PID and reverse step control, a variable PID tuning method is proposed [26]. A back-stepping control gain tuning method is designed using a combination of nominal gain and variable gain to adjust the desired transient performance [27]. Although these methods are proposed for intuitive self-learning gain, the stability analysis of adaptive tuning gain is not enough.

In this paper, we propose an AAN controller with adaptive gain for nonlinear systems with unknown external time-varying perturbations: The controller uses the backstepping method to track the target trajectory, and directly adjusts the output of the controller by tracking performance to obtain AAN characteristics. The adaptive law is used to update the control gain to suppress the tracking error within the expected range to obtain satisfactory control performance without interference information. The upper bound residuals of unknown perturbations are updated synchronously around the desired boundary, and the control gain is adjusted to avoid unnecessary high gains when the residuals set is less than the desired boundary.

The main contributions of this paper are:

1. Through the dynamic gain adjustment mechanism, the system can feedback and adjust the control force in real-time, avoiding excessive or insufficient assistance, and helping to adapt to the problem of reduced auxiliary accuracy caused by internal or external interference in the rehabilitation training process.

2. The dynamic adaptation mechanism is used to further solve the transient instability effects at the nodes of dynamic adjustment on demand, overcome the problem that traditional adaptive cannot efficiently identify dynamic changing parameters, and realize the adaptive adjustment of auxiliary strength and mode according to the specific situation and progress of the convalescent

3. The adaptive AAN gain control proposed in this paper avoids the problem that the traditional high-gain adaptive control may cause the dynamic adaptive ability of

on-demand assistance to be too sensitive, reduces overshoot and steady-state shock, and ensures the safety and comfort of rehabilitation training.

II. THE EQUATION OF MOTION OF THE ROBOT

The robotic exoskeleton mentioned above is described by a common second-order Euler-Lagrange dynamic model in the Cartesian coordinate system, as shown in equation (1) [28]:

$$M_x(x)\ddot{x} + C(x,\dot{x})\dot{x} + G(x) + F(\dot{x}) = J^{-T}\tau + f_{ext} \quad (1)$$

This model can also be written as formula (2) in the joint coordinate system.

$$M(q)\ddot{q} + C(q,\dot{q})\dot{q} + G(q) + F(\dot{q}) = \tau + J^T f_{ext} \quad (2)$$

In formula (1), $x \in \mathbb{R}^n$, $\dot{x} \in \mathbb{R}^n$, and $\ddot{x} \in \mathbb{R}^n$ respectively represent the robot end position, velocity and acceleration, n is the number of rigid linkages in the robot model;

In formula (2), $q \in \mathbb{R}^n$, $\dot{q} \in \mathbb{R}^n$, and $\ddot{q} \in \mathbb{R}^n$ respectively represent the angular position, angular velocity, and angular acceleration of each joint; $M(q) \in \mathbb{R}^{n\times n}$ is rigid body inertia matrix; $C(q,\dot{q}) \in \mathbb{R}^{n\times n}$ are centrifugal force and Coriolis force matrix; $G(q) \in \mathbb{R}^n$ is robot gravity torque, $F(\dot{q}) \in \mathbb{R}^n$ is friction and other disturbances, $\tau \in \mathbb{R}^n$ is the control input and $f_{ext} \in \mathbb{R}^n$ is expressed as the robot-environment interaction force; $\dot{x} = J(q)\dot{q}$, $J(q) \in \mathbb{R}^{n\times n}$ is a Jacobian matrix and is non-singular, satisfying:

$$\begin{aligned} M_x(x) &\triangleq J^{-T}M(q)J^{-1}, \\ C_x(x,\dot{x}) &\triangleq J^{-T}[C_q(q,\dot{q}) - M(q)J^{-1}\dot{J}]J^{-1}, \\ G_x(x) &\triangleq J^{-T}G(q), \quad F_x(\dot{x}) = J^{-T}F(\dot{q}) \end{aligned}$$

The robot in equation (2) has the following properties:

Property 1: $M(q)$ is a positive definite matrix and satisfies the following relation:

$\underline{M}I \le M(q) \le \overline{M}I$, I is the identity matrix of $n \times n$, $\underline{M}$ and $\overline{M}$ representing the smallest eigenvalue and the largest eigenvalue respectively.

In order to make the subsequent simulation experiments more in line with the physical reality, the model satisfies the following assumptions:

Assumption 1: Joint misalignment between the wearable robot and the subject during movement can be compensated by the robot.

Assumption 2: Considering that the robot joint has a physical limit, the controller input torque limit is set to $\pm 22\ N \cdot m$ in the simulation.

III. CONTROLLER DESIGN

In this section, an AAN control scheme based on adaptive learning gain is proposed, which adjusts the controller performance according to the trajectory tracking error to realize the on-demand auxiliary function, that is, it only provides strong help when the patient cannot complete the predetermined trajectory movement and reduces the help when the patient has sufficient ability. Similar methods have been used in some previous literature, and the advantage of the controller proposed in this paper is that it adopts a nonlinear control method based on adaptive learning gain (ALG) without any information about interference and gain tuning, which restrains the tracking error within the desired range.

$$e = q_d - q \quad (3)$$

where q_d is the reference position of the given joint, q is the actual motion position of the joint, and e is the error of the joint position.

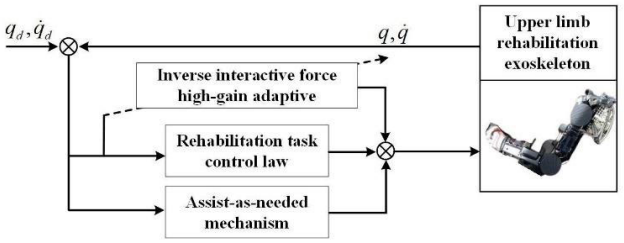

FIGURE 1. Control strategy block diagram.

Note 1: For better tracking performance in trajectory tracking problems, it is difficult to ensure the convergence of $e, \dot{e}, \ddot{e}$. So, we define a new error r, which has the following formula:

$$r = k_1 e + k_2 \dot{e} \quad (4)$$

If r and $\dot{r}$ both converge to zero as $t \to \infty$, then $e, \dot{e}, \ddot{e}$ both converge to 0 as $t \to \infty$, where both k_1 and k_2 are constant gains and both are positive numbers.

Combined with formulas (2), (3),and (4), the following dynamic model about r can be obtained:

$$\begin{aligned} M(q)\dot{r} = M(q)(k_2\ddot{q}_r + k_1\dot{e}) - k_2 C(q,\dot{q})r \\ - k_2(\tau + J^T f_{ext}) + k_2(G(q) + F(\dot{q})) \end{aligned} \quad (5)$$

The control law design is:

$$\begin{aligned} \tau = C(q,\dot{q})r + M(q)(k_1\dot{e} + k_2\ddot{q}_r + \hat{k}r \\ + k_3 \mathrm{Tanh}(\chi(r,\gamma)))/k_2 + G(q) \end{aligned} \quad (6)$$

where $\hat{k}$ is the estimate of the adaptive learning gain that has not been set. k_3, γ is constant.

Substituting the control law (6) into equation (5) gives the closed-loop dynamics of the error:

$$M(q)\dot{r} = -\hat{k}r - k_3 \mathrm{Tanh}(\chi(r,\gamma)) + k_2 F(\dot{q}) - J^T f_{ext} \quad (7)$$

In the formula:

$$\chi(r,\gamma) = \begin{cases} 0, & |r| < \gamma \\ r - \gamma\, sign(r), & |r| > \gamma \end{cases} \quad (8)$$

and

$$\varepsilon = k_2 F(\dot{q}) - J^T f_{ext} \quad (9)$$

If ε is regarded as a disturbance in trajectory tracking, then (7) can be rewritten as:

$$M(q)\dot{r} = -\hat{k}r + k_3\text{Tanh}(\chi(r,\gamma)) + \varepsilon \tag{10}$$

Assumption 3: The unknown time-varying positive ideal gain $K^*(t)$ exists and satisfies the following relations:

$$K^*(t) > \hat{k}(t),\ \underline{K}^* \leqslant K^*(t) \leqslant \overline{K}^*,\ \sup\left|\dot{K}^*(t)\right| = \kappa$$

where $\overline{K}^*$, $\underline{K}^*$, κ are positive constants, if $\hat{k}$ in formula (9) can be replaced by $K^*(t)$, then $K^*(t)$ can be adjusted according to the influence of perturbation, to ensure that the error changes within the expected range θ:

The update rate of the adaptive learning gain is designed as follows:

$$\dot{\hat{k}} = \begin{cases} \lambda_1 r^2 sign(|r| - \theta), & \hat{k} > k_{\min} \\ \varphi, & \hat{k} = k_{\min} \end{cases} \tag{11}$$

λ_1 is the learning rate, and $\lambda_1 > 1$, φ is a small constant, θ is also a small constant as an error boundary, the initial value of $\hat{k}$ is greater than k_{min}, k_{min} is also a positive number.

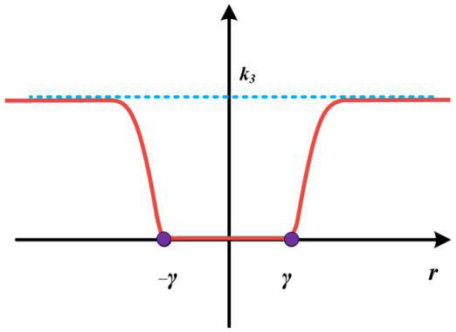

FIGURE 2. Modulation term with AAN performance.

Note 2: In the update rate of adaptive learning gain, when the error is less than θ, the gain keeps increasing; When the error is within the allowable range, that is $r < \theta$, the learning gain is kept at the lowest level;

Assumption 4: $F(\dot{q})$ is an external disturbance, and there is an upper bound, which is: $\delta = sup\,|F(\dot{q})|$.

Theorem 1: Consider hypotheses 1-4, for the control input (7) and the adaptive law (10), the tracking error and the control gain estimation error $\tilde{k} = K^* - \hat{k}$, both bounded as follows [12]:

$$\lim_{t\to\infty} V_1(t) \leq \frac{h_1}{b_1} \tag{12}$$

where

$$\begin{aligned} V_1 &= \frac{1}{2}r^2 + \frac{1}{2}\tilde{k}^2 \\ b_1 &= \min\left(2\left(\underline{K}^* - \frac{1}{\mu}\right), 2\alpha\theta^2\right) \\ h_1 &= \alpha\theta^2\tilde{k}_{\max}^2 + \tilde{k}_{\max}\theta^2\beta + \frac{\mu}{4}\delta^2 + \tilde{k}_{\max}\kappa \end{aligned} \tag{13}$$

where α, β, μ are positive constants that will be used in the following proof.

Proof: The Lyapunov function is defined as:

$$V_1 = \frac{1}{2}r^2 + \frac{1}{2}\tilde{k}^2 \tag{14}$$

Derivation of equation (14) gives (15):

$$\begin{aligned} \dot{V}_1 &= r\left(F(q) - \hat{k}r - k_3\,\text{Tanh}(\chi(r,\gamma))\right) \\ &\quad + \tilde{k}\dot{K}^* - \tilde{k}\dot{\hat{k}} \\ &= F(q)r - \hat{k}r^2 - k_3\,\text{Tanh}(\chi(r,\gamma))r \\ &\quad + \tilde{k}\dot{K}^* - \tilde{k}\lambda_1 r^2\,\text{sign}(|r| - \theta) \end{aligned} \tag{15}$$

According to the symbol of $(|r| - \theta)$, it can be divided into two cases:

(1) Case 1: When $|r| > \theta$, (15) can be arranged as:

$$\begin{aligned} \dot{V}_1 &= F(q)r - \hat{k}r^2 - \tilde{k}\lambda_1 r^2 + \tilde{k}\dot{K}^* - k_3\,\text{Tanh}(\chi(r,\gamma))r \\ &= -\hat{k}r^2 - \tilde{k}\lambda_1 r^2 + K^*r^2 - K^*r^2 + \alpha r^2\tilde{k}^2 - \alpha r^2\tilde{k}^2 \\ &\quad + F(q)r + \tilde{k}\dot{K}^* - k_3\,\text{Tanh}(\chi(r,\gamma))r \\ &= -K^*r^2 - \alpha r^2\tilde{k}^2 - \tilde{k}r^2(\lambda_1 - 1 - \alpha\tilde{k}) + F(q)r \\ &\quad + \tilde{k}\dot{K}^* - k_3\,\text{Tanh}(\chi(r,\gamma))r \end{aligned} \tag{16}$$

α is a positive constant, and α satisfies the condition of $\alpha < ((\lambda_1 - 1)/\tilde{k}_{\max}) < ((\lambda_1 - 1)/\tilde{k})$, $\tilde{k}_{\max}$ is constant and $\tilde{k}_{\max} = K^* - k_{\min}$.

Formula (16) can be further rewritten as:

$$\begin{aligned} \dot{V}_1 &\leqslant -\underline{K}^*r^2 - \alpha r^2\tilde{k}^2 - \underbrace{\tilde{k}r^2\left(\lambda_1 - 1 - \alpha\tilde{k}\right)}_{>0} \\ &\quad + F(q)r + \tilde{k}\dot{\underline{K}}^* - k_3\,\text{Tanh}(\chi(r,\gamma))r \\ &\leqslant -\underline{K}^*r^2 - \alpha r^2\tilde{k}^2 + \frac{1}{\mu}r^2 + \frac{\mu}{4}\delta^2 \\ &\quad + \tilde{k}_{\max}\kappa - k_3\,\text{Tanh}(\chi(r,\gamma))r \\ &\leqslant -(\underline{K}^* - \frac{1}{\mu})r^2 - \alpha\theta^2\tilde{k}^2 + \frac{\mu}{4}\delta^2 \\ &\quad + \tilde{k}_{\max}\kappa - k_3\,\text{Tanh}(\chi(r,\gamma))r \\ &\leqslant -\underbrace{\min\left(2\left(\underline{K}^* - \frac{1}{\mu}\right), 2\alpha\theta^2\right)}_{=b_1}\frac{1}{2}(r^2 + \tilde{k}^2) \\ &\quad + \underbrace{\frac{\mu}{4}\delta^2 + \tilde{k}_{\max}\kappa}_{=s_1} - k_3\,\text{Tanh}(\chi(r,\gamma))r \\ &\leqslant -b_1V_1 + s_1 - k_3\,\text{Tanh}(\chi(r,\gamma))r \end{aligned} \tag{17}$$

where b_1, s_1, μ are positive constant terms, and μ satisfies the condition: $\mu > (1/\underline{K}^*)$

(2) Case 2: When $|r| < \theta$, (15) can be arranged as:

$$\begin{aligned} \dot{V}_1 &= F(q)r - \hat{k}r^2 + \tilde{k}\lambda_1 r^2 + \tilde{k}\dot{K}^* - k_3\,\text{Tanh}(\chi(r,\gamma))r \\ &= -\hat{k}r^2 + \tilde{k}\lambda_1 r^2 + K^*r^2 - K^*r^2 + \alpha r^2\tilde{k}^2 - \alpha r^2\tilde{k}^2 \\ &\quad + F(q)r + \tilde{k}\dot{K}^* - k_3\,\text{Tanh}(\chi(r,\gamma))r \\ &= -K^*r^2 - \alpha r^2\tilde{k}^2 + \tilde{k}r^2(\lambda_1 + 1 + \alpha\tilde{k}) \\ &\quad + F(q)r + \tilde{k}\dot{K}^* - k_3\,\text{Tanh}(\chi(r,\gamma))r \end{aligned} \tag{18}$$

Similarly, α is a positive constant, and α satisfies the condition of $\alpha < ((\lambda_1 - 1)/\tilde{k}_{\max}) < ((\lambda_1 - 1)/\tilde{k})$, $\tilde{k}_{\max}$ is constant and $\tilde{k}_{\max} = K^* - k_{\min}$.

Formula (18) can be rewritten as:

$$\begin{aligned}
\dot{V}_1 &\leqslant -\underline{K}^* r^2 - \alpha r^2 \tilde{k}^2 + \underbrace{\tilde{k}_{\max} r^2 \left(\lambda_1 + 1 + \alpha \tilde{k}_{\max}\right)}_{>0} \\
&\quad + F(q)r + \tilde{k}_{\max}\kappa - k_3 \operatorname{Tanh}(\chi(r,\gamma))r \\
&\leqslant -\underline{K}^* r^2 - \underbrace{\alpha r^2 \tilde{k}^2}_{>0} + \tilde{k}_{\max}\theta^2\beta + \frac{1}{\mu}r^2 + \frac{\mu}{4}\delta^2 \\
&\quad + \tilde{k}_{\max}\kappa - k_3 \operatorname{Tanh}(\chi(r,\gamma))r \\
&\leqslant -(\underline{K}^* - \frac{1}{\mu})r^2 - \alpha\theta^2\tilde{k}^2 + \alpha\theta^2\tilde{k}^2 + \tilde{k}_{\max}\theta^2\beta \\
&\quad + \frac{\mu}{4}\delta^2 + \tilde{k}_{\max}\kappa - k_3 \operatorname{Tanh}(\chi(r,\gamma))r \\
&\leqslant -\underbrace{\min\left(2\left(\underline{K}^* - \frac{1}{\mu}\right), 2\alpha\theta^2\right)}_{=b_1} \frac{1}{2}(r^2 + \tilde{k}^2) \\
&\quad + \underbrace{\alpha\theta^2\tilde{k}^2 + \tilde{k}_{\max}\theta^2\beta + s_1}_{h_1} - k_3 \operatorname{Tanh}(\chi(r,\gamma))r \\
&\leqslant -b_1 V_1 + h_1 - k_3 \operatorname{Tanh}(\chi(r,\gamma))r \qquad (19)
\end{aligned}$$

Considering the above two cases, V_1 can be rewritten as:

$$\begin{aligned}
\dot{V}_1 &\leqslant -b_1 V_1 + \max(s_1, h_1) - k_3 \operatorname{Tanh}(\chi(r,\gamma))r \\
&\leqslant -b_1 V_1 + h_1 - k_3 \operatorname{Tanh}(\chi(r,\gamma))r \qquad (20)
\end{aligned}$$

When $\|r\| \geq \gamma$:

$$\begin{aligned}
\dot{V}_2 &\leqslant -rk_3 \tanh(r - \gamma sign(r)) \\
&\leqslant -rk_3[\frac{\tanh(r) - \tanh(\gamma sign(r))}{1 + \tanh(r)\tanh(\gamma sign(r))}] \\
&\leqslant -rk_3[k_r(\tanh(r) - \tanh(\gamma sign(r)))] \\
&\leqslant -rk_3k_r \tanh(r) + rk_3k_r \tanh(\gamma sign(r)) \\
&\leqslant -k_3k_r \|r\| + 0.2785k_3k_r \\
&\quad + rk_3k_r \tanh(\gamma sign(r)) \qquad (21)
\end{aligned}$$

We can easily obtain (22)(23) by using the absolute value inequality:

$$rk_3k_r \tanh(\gamma sign(r)) \leq \|r\| k_3k_r \qquad (22)$$

where: $k_r = \frac{1}{1+\tanh(r)\tanh(\gamma sign(r))}$, $0 < k_r \leq 2$

$$\begin{aligned}
\dot{V}_2 &\leqslant -k_3k_r \|r\| + 0.2785k_3k_r + \|r\| k_3k_r \\
&\leqslant 0.557k_3 \qquad (23)
\end{aligned}$$

From formula (20) and formula (23), it can be obtained:

$$\dot{V}_1 \geq -b_1 V_1 + h_1 \qquad (24)$$

When $\|r\| \leq \gamma$, Obviously $k_3 \operatorname{Tanh}(\chi(r,\gamma))r$ is 0, so formula (24) is also satisfied.

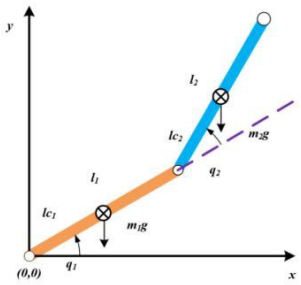

FIGURE 3. Schematic diagram of a simplified exoskeleton model.

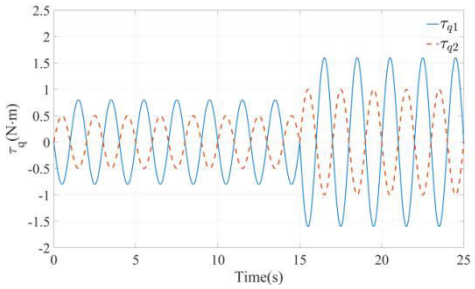

FIGURE 4. Time-varying interaction force Settings between system and environment.

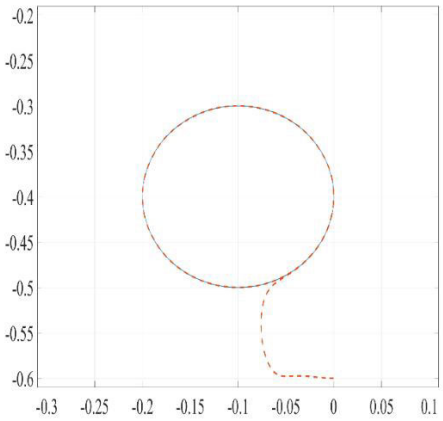

FIGURE 5. Adaptive gain AAN controller terminal trajectory.

IV. SIMULATION

A. SIMULATION DESIGN AND MODEL BUILDING

Because the degrees of freedom of the upper limb exoskeleton designed at home and abroad are not the same, the shoulder joint uses 1-3 degrees of freedom, and the elbow joint uses one degree of freedom. To make the control algorithm widely used in various exoskeletons, only flexion and extension degrees of freedom are reserved for elbow joints and shoulder joints. Then this model can be represented by two links and used in simulation and experimental model building. The two-link model is shown in Figure 3. The structural parameters of the model are as follows:

$$m_1 = 20kg,\ l_1 = 0.3\ m,\ Iz_1 = 0.45\ kg \cdot m^2,\ Ic_1 = 0.15m;$$
$$m_2 = 20kg,\ l_2 = 0.3\ m, Iz_2 = 0.45\ kg \cdot m^2,\ Ic_2 = 0.15m;$$

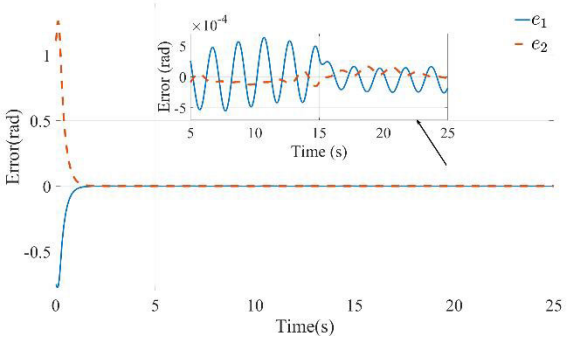

FIGURE 6. Adaptive gain AAN controller joint error.

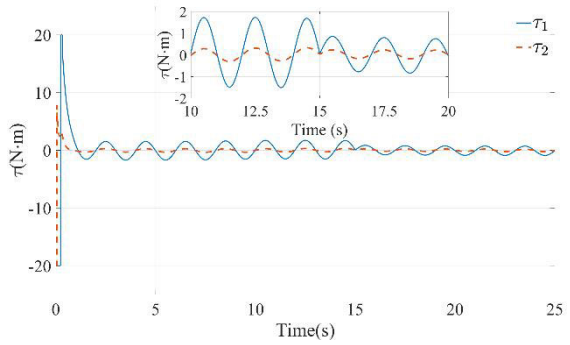

FIGURE 7. Adaptive gain AAN controller joint output torque.

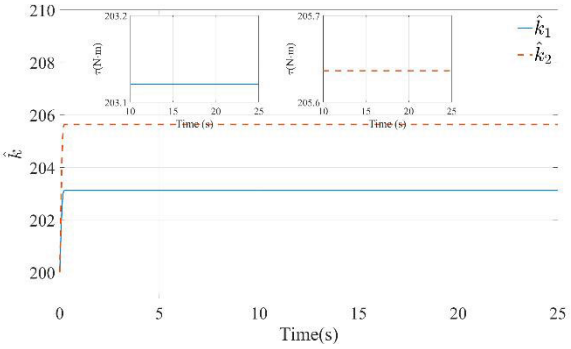

FIGURE 8. Adaptive gain.

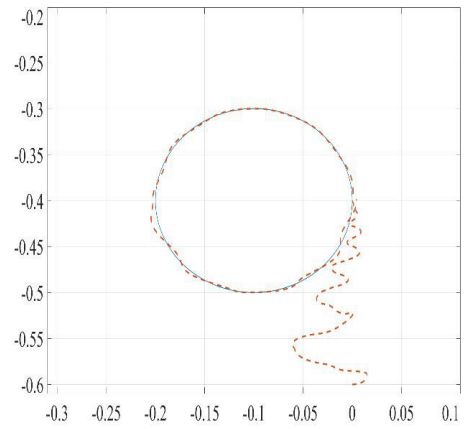

FIGURE 9. Impedance AAN controller terminal trajectory.

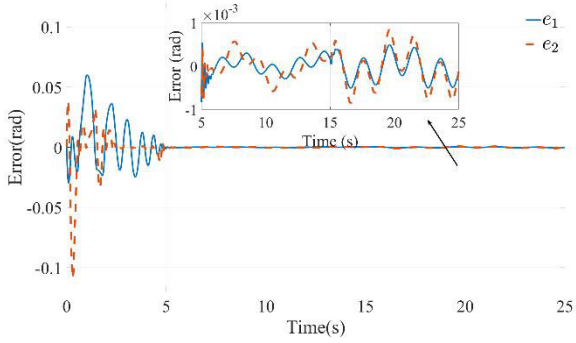

FIGURE 10. Impedance AAN controller joint error.

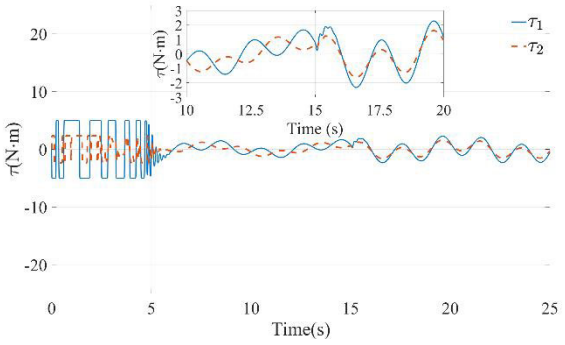

FIGURE 11. Impedance AAN controller joint output torque.

where m_1 and m_2 are the upper arm and forearm model masses respectively; l_1 and l_2 are the upper arm and forearm model lengths respectively; Iz_1 and Iz_2 are the upper arm and forearm model inertial moments respectively;

Ic_1 and Ic_2 are the center of gravity positions of upper arm and forearm model respectively;

Considering the patient's insufficient ability to move limbs, the trajectory in the simulation was set as a small circular trajectory common in daily life. The center position of the circle is $(-0.1, -0.4)$, the radius of the circle is $0.1m$, and the error disturbance value is assumed to be: $d = 0.8\sin(\pi t)$, and the simulation is set in the horizontal plane, so the influence of gravity is ignored.

In the simulation, the simplified exoskeleton model needs to complete the trajectory tracking task, and the simulation time is set to 25 seconds. In the first 15 seconds, a small time-varying external force is set to simulate the real environment, and after 15 seconds, the external force is mutated to a larger time-varying value.

According to formula (2), the torque of external forces on joints in joint space needs to be mapped through the Jacobian matrix, so we can directly set the value after mapping

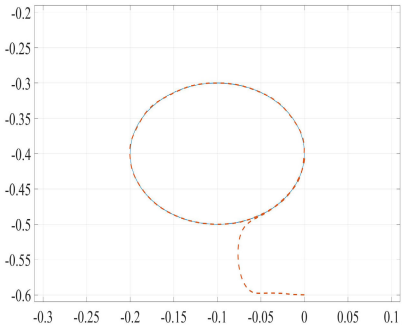

FIGURE 12. Recent AAN controller terminal trajectory.

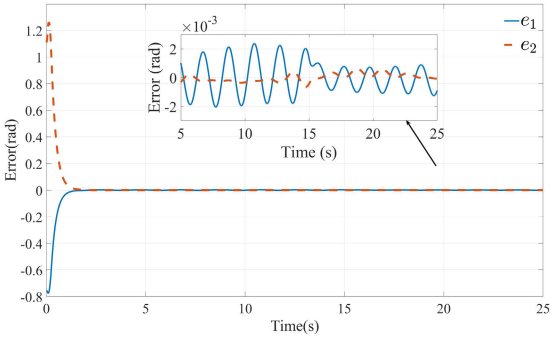

FIGURE 13. Recent AAN controller joint error.

as follows:

$$J^T f_{ext} = \begin{bmatrix} \tau_{q_1} \\ \tau_{q2} \end{bmatrix}$$

where τ_{q_1} and τ_{q2} are the mappings of the environmental interaction forces to the two joints respectively, and their values are set as shown in Figure 4:

$$\tau_{q_1} = \begin{cases} -0.8\sin(\pi t), & 0 < t < 15 \\ 1.6\sin(\pi t), & 15 < t < 25 \end{cases}$$

$$\tau_{q2} = \begin{cases} 0.5\sin(\pi t), & 0 < t < 15 \\ \sin(\pi t), & 15 < t < 25 \end{cases}$$

B. SIMULATION RESULT

Impedance on Demand controller and adaptive gain on Demand controller were used for simulation. The two kinds of simulation used the same model to compare and verify the adaptive ability of the adaptive gain-on-demand controller to the interaction time-varying force and the flexibility of motion.

The controller parameters are as follows:

$$k_1 = 2, k_2 = 0.5, k_3(q_1) = 1.55, k_3(q_2) = 2.35,$$
$$\gamma = 0.0001,\ \lambda_1(q_1) = 8,\ \lambda_1(q_2) = 4,\ \theta = 0.001,$$
$$k_{\min} = 170,\ \varphi = 0.1;$$

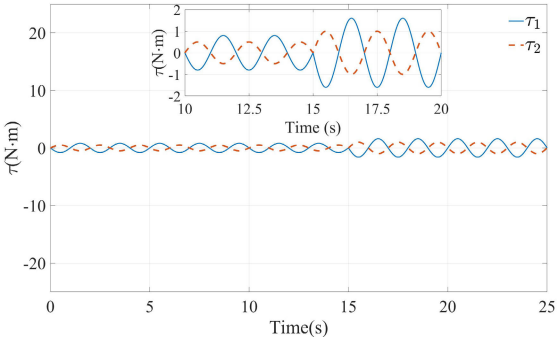

FIGURE 14. Recent AAN controller joint output torque.

From the point of view of the error, the error quickly converges, in the case of the external torque increased by the joint, although the error is slightly increased, it can still rapidly converge, and the controller has good adaptability. When the external torque on the joint is increased, the torque provided by the controller is significantly reduced to avoid excessive assistance.

The adaptive controller proposed in the paper [28] can also effectively overcome the problem of over-estimation of gain caused by conventional static modulation and improve the model's adaptive ability to complex environments.

$$\dot{\hat{k}} = \begin{cases} \lambda_1 \sqrt{\frac{\gamma_1}{2}} sign(|r| - \theta), & \hat{k} > k_{\min} \\ \varphi, & k \le k_{\min} \end{cases} \tag{25}$$

where $\lambda_1, \gamma_1, \theta, \varphi$ and $k_{\min}$ are positive constants.

After replacing the adaptive law in the algorithm with the adaptive law mentioned in the paper [29], the results are obtained as shown in the figures below. It can be observed that the algorithm can still approximate the reference trajectory and still has a certain adaptive ability to external disturbances. However, the error is larger than the previous algorithm and the stability is not as good as the algorithm proposed in this paper, so it can be proved that the algorithm proposed in this paper has good robustness and adaptive ability.

The simulation results show that the impedance controller achieves good trajectory tracking performance, but it is not sensitive to the change of environmental interaction force, and the torque provided by the controller does not change significantly. By contrast, it can be shown that the adaptive gain on-demand controller can respond to the environmental interaction time-varying force, and further ensures the flexibility of motion.

V. CONCLUSION

To solve the AAN control problem of the upper limb exoskeleton, we proposed an AAN controller with adaptive gain for the existing rod-driven exoskeleton. Through the dynamic gain adjustment mechanism, the system can adjust the control force with real-time feedback, avoiding excessive or insufficient assistance. It also helps to adapt to the problem

of decreasing auxiliary accuracy caused by internal or external interference in the rehabilitation training process and improves the safety and comfort of rehabilitation training.The simulation results and comparative experiments show that this controller has better disturbance rejection characteristics compared to ordinary adaptive gain controllers. And in the case of sudden disturbances, it is better to adjust the degree of assistance and ensure tracking error. Based on the research results of this paper, the algorithm can be applied to a wider range of patient rehabilitation in the future.

REFERENCES

[1] A. G. Thrift, D. A. Cadilhac, T. Thayabaranathan, G. Howard, V. J. Howard, P. M. Rothwell, and G. A. Donnan, "Global stroke statistics," *Int. J. Stroke*, vol. 9, no. 1, pp. 6–18, Dec. 2013, doi: 10.1111/ijs.12245.

[2] M. M. Mirbagheri, C. Tsao, and W. Z. Rymer, "Recovery of arm movement after stroke," in *Proc. 29th Annu. Int. Conf. IEEE Eng. Med. Biol. Soc.*, Aug. 2007, pp. 5370–5372, doi: 10.1109/IEMBS.2007.4353555.

[3] F. C. Huang and J. L. Patton, "Augmented dynamics and motor exploration as training for stroke," *IEEE Trans. Biomed. Eng.*, vol. 60, no. 3, pp. 838–844, Mar. 2013, doi: 10.1109/TBME.2012.2192116.

[4] G. Herrnstadt, N. Alavi, J. Neva, L. A. Boyd, and C. Menon, "Preliminary results for a force feedback bimanual rehabilitation system," in *Proc. 6th IEEE Int. Conf. Biomed. Robot. Biomechatronics (BioRob)*, Singapore, Jun. 2016, pp. 768–773.

[5] J. L. Pons, *Wearable Robots: Biomechatronic Exoskeletons*. Chichester, U.K.: Wiley, 2008.

[6] C. Carignan, J. Tang, S. Roderick, and M. Naylor, "A configuration-space approach to controlling a rehabilitation arm exoskeleton," in *Proc. IEEE 10th Int. Conf. Rehabil. Robot.*, Jun. 2007, pp. 179–187, doi: 10.1109/ICORR.2007.4428425.

[7] Y. Zimmermann, A. Forino, R. Riener, and M. Hutter, "ANYexo: A versatile and dynamic upper-limb rehabilitation robot," *IEEE Robot. Autom. Lett.*, vol. 4, no. 4, pp. 3649–3656, Oct. 2019, doi: 10.1109/LRA.2019.2926958.

[8] T. Nef, M. Guidali, and R. Riener, "ARMin III—Arm therapy exoskeleton with an ergonomic shoulder actuation," *Appl. Bionics Biomech.*, vol. 6, no. 2, pp. 127–142, Jul. 2009, doi: 10.1080/11762320902840179.

[9] J. C. Perry, J. Rosen, and S. Burns, "Upper-limb powered exoskeleton design," *IEEE/ASME Trans. Mechatronics*, vol. 12, no. 4, pp. 408–417, Aug. 2007, doi: 10.1109/TMECH.2007.901934.

[10] B. Dehez and J. Sapin, "ShouldeRO, an alignment-free two-DOF rehabilitation robot for the shoulder complex," in *Proc. IEEE Int. Conf. Rehabil. Robot.*, Jun. 2011, pp. 1–8, doi: 10.1109/ICORR.2011.5975339.

[11] Z. Warraich and J. A. Kleim, "Neural plasticity: The biological substrate for neurorehabilitation," *PM R*, vol. 2, no. 12, pp. S208–S219, Dec. 2010, doi: 10.1016/j.pmrj.2010.10.016.

[12] H. J. Asl, M. Yamashita, T. Narikiyo, and M. Kawanishi, "Field-based assist-as-needed control schemes for rehabilitation robots," *IEEE/ASME Trans. Mechatronics*, vol. 25, no. 4, pp. 2100–2111, Aug. 2020, doi: 10.1109/TMECH.2020.2992090.

[13] H. J. Asl, T. Narikiyo, and M. Kawanishi, "An assist-as-needed control scheme for robot-assisted rehabilitation," in *Proc. Amer. Control Conf. (ACC)*, May 2017, pp. 198–203, doi: 10.23919/ACC.2017.7962953.

[14] Y. Guo, Y. Tian, H. Wang, and S. Han, "Adaptive hybrid-mode assist-as-needed control of upper limb exoskeleton for rehabilitation training," *Mechatronics*, vol. 100, Jun. 2024, Art. no. 103188, doi: 10.1016/j.mechatronics.2024.103188.

[15] Y. Wang, Y. Guo, Y. Tao, Y. Tian, and H. Wang, "Human-centered active torque-based AAN impedance control for lower limb patient-exoskeleton coupling system in the rehabilitation," *Int. J. Robust Nonlinear Control*, pp. 1–36, Sep. 2023, doi: 10.1002/rnc.6996. [Online]. Available: https://onlinelibrary.wiley.com/doi/abs/10.1002/rnc.6996#

[16] Y. Tian, Y. Guo, H. Wang, and D. G. Caldwell, "Training task planning-based adaptive assist-as-needed control for upper limb exoskeleton using neural network state observer," *Neural Comput. Appl.*, May 2024, doi: 10.1007/s00521-024-09922-5. [Online]. Available: https://link.springer.com/article/10.1007/s00521-024-09922-5#citeas

[17] W. Shaw Cortez, D. Oetomo, C. Manzie, and P. Choong, "Control barrier functions for mechanical systems: Theory and application to robotic grasping," *IEEE Trans. Control Syst. Technol.*, vol. 29, no. 2, pp. 530–545, Mar. 2021, doi: 10.1109/TCST.2019.2952317.

[18] L. Liu, T. Gao, Y.-J. Liu, S. Tong, C. L. P. Chen, and L. Ma, "Time-varying IBLFs-based adaptive control of uncertain nonlinear systems with full state constraints," *Automatica*, vol. 129, Jul. 2021, Art. no. 109595, doi: 10.1016/j.automatica.2021.109595.

[19] W. Kim, X. Chen, Y. Lee, C. C. Chung, and M. Tomizuka, "Discrete-time nonlinear damping backstepping control with observers for rejection of low and high frequency disturbances," *Mech. Syst. Signal Process.*, vol. 104, pp. 436–448, May 2018, doi: 10.1016/j.ymssp.2017.11.006.

[20] R. Q. Fuentes-Aguilar and I. Chairez, "Adaptive tracking control of state constraint systems based on differential neural networks: A barrier Lyapunov function approach," *IEEE Trans. Neural Netw. Learn. Syst.*, vol. 31, no. 12, pp. 5390–5401, Dec. 2020, doi: 10.1109/TNNLS.2020.2966914.

[21] I. S. Dimanidis, C. P. Bechlioulis, and G. A. Rovithakis, "Output feedback approximation-free prescribed performance tracking control for uncertain MIMO nonlinear systems," *IEEE Trans. Autom. Control*, vol. 65, no. 12, pp. 5058–5069, Dec. 2020, doi: 10.1109/TAC.2020.2970003.

[22] Y. Hwang, C. M. Kang, and W. Kim, "Robust nonlinear control using barrier Lyapunov function under lateral offset error constraint for lateral control of autonomous vehicles," *IEEE Trans. Intell. Transp. Syst.*, vol. 23, no. 2, pp. 1565–1571, Feb. 2022, doi: 10.1109/TITS.2020.3023617.

[23] H. Huang, W. He, J. Li, B. Xu, C. Yang, and W. Zhang, "Disturbance observer-based fault-tolerant control for robotic systems with guaranteed prescribed performance," *IEEE Trans. Cybern.*, vol. 52, no. 2, pp. 772–783, Feb. 2022, doi: 10.1109/TCYB.2019.2921254.

[24] H. K. Khalil, "High-gain observers in feedback control: Application to permanent magnet synchronous motors," *IEEE Control Syst. Mag.*, vol. 37, no. 3, pp. 25–41, Jun. 2017, doi: 10.1109/MCS.2017.2674438.

[25] J.-W. Jung, V. Q. Leu, T. D. Do, E.-K. Kim, and H. H. Choi, "Adaptive PID speed control design for permanent magnet synchronous motor drives," *IEEE Trans. Power Electron.*, vol. 30, no. 2, pp. 900–908, Feb. 2015, doi: 10.1109/TPEL.2014.2311462.

[26] J. Y. Lee, M. Jin, and P. H. Chang, "Variable PID gain tuning method using backstepping control with time-delay estimation and nonlinear damping," *IEEE Trans. Ind. Electron.*, vol. 61, no. 12, pp. 6975–6985, Dec. 2014, doi: 10.1109/TIE.2014.2321353.

[27] D. X. Ba, H. Yeom, J. Kim, and J. Bae, "Gain-adaptive robust backstepping position control of a BLDC motor system," *IEEE/ASME Trans. Mechatronics*, vol. 23, no. 5, pp. 2470–2481, Oct. 2018, doi: 10.1109/TMECH.2018.2864187.

[28] S. You and W. Kim, "Adaptive learning gain-based control for nonlinear systems with external disturbances: Application to PMSM," *IEEE Trans. Control Syst. Technol.*, vol. 31, no. 3, pp. 1427–1434, May 2023, doi: 10.1109/TCST.2022.3208446.

[29] M. K. Khan, "Design and application of second order sliding mode control algorithms," Univ. Leicester, 2003. [Online]. Available: https://lra.le.ac.uk/bitstream/2381/30209/1/U180131.pdf

JIXIN DONG was born in Harbin, Heilongjiang, in 1999. He received the bachelor's degree in engineering from Northeast Agricultural University, in 2021. He is currently pursuing the degree with Yanshan University, with a primary research focus on structural design and control of upper limb exoskeletons. Additionally, he has been granted two patents for his work.

ZHIWEI JIA was born in Hengshui, Hebei, in 1999. He received the bachelor's degree from the Liren College, Yanshan University, in 2021, and the master's and Ph.D. degrees from Yanshan University, in 2021 and 2023, respectively.

ERWEI LI was born in October 1987. He received the Ph.D. degree in engineering with a major in mechanical and electronic engineering from Yanshan University, in June 2018. He is currently a member of the Communist Party of China. His main research interest includes the theoretical research and application of marine parallel heavy stabilization equipment. Following this, he was the Team Secretary of ''Basic Theory of Parallel Equipment and Integration of Mechanical and Electrical Systems'' with the School of Mechanical Engineering, Yanshan University, from July 2018 to March 2019, where he has been an Associate Professor with the Department of Mechanical and Electronic Engineering, School of Mechanical Engineering, since April 2019. To date, he has published 21 articles and been granted 18 patents.

QIPENG LV received the master's degree in precision instruments and machinery from Shenyang University of Technology. Currently, he engaged in the research of the new generation information technology with the Second Research Institute of China Electronics Technology Group Corporation.